

# Judging the Generalized Newtonian Fluid assumption for cuttings transport modelling by applying time scale comparisons

Alexander Busch<sup>1</sup>, Stein Tore Johansen<sup>1,2</sup>

<sup>1</sup>Norwegian University of Science and Technology (NTNU), Trondheim, Norway

<sup>2</sup>SINTEF Materials and Chemistry, Trondheim, Norway

\*Corresponding author: [alexander.busch@ntnu.no](mailto:alexander.busch@ntnu.no), [alexander.busch@alumni.ntnu.no](mailto:alexander.busch@alumni.ntnu.no)

## ABSTRACT

In drilling research, aqueous Polyanionic Cellulose (PAC) solutions are often employed as drilling fluid model systems in experimental laboratory studies to investigate cuttings transport. For this purpose, PAC solutions are typically assumed to behave purely viscous, i.e. they do not show time-dependent/thixotropic and/or viscoelastic properties and are thus modelled with a Generalized Newtonian Fluid (GNF) constitutive equation. However, PAC solutions feature both viscoelastic and thixotropic properties on different time scales<sup>1</sup>. In this study, cuttings transport process time scales are compared with rheological time scales for PAC solutions<sup>1</sup>. Using the concepts of Deborah and Weissenberg numbers as well as Pipkin spaces for two spatial scales, an arbitrary annular (wellbore) section and the particle scale, we show that PAC solutions may not necessarily satisfy a GNF formulation under all circumstances. In particular, for Lagrangian unsteady flows, e.g. due to flow start-up, particle acceleration and/or spatially developing flows, the GNF framework is not entirely valid and leads to some error. We suggest several actions to minimize the magnitude of the error.

## NOMENCLATURE

Throughout the manuscript, we apply the official nomenclature of The Society of Rheology<sup>2</sup>, unless indicated otherwise and with the following additional definitions.

## Abbreviations

CMC	Carboxymethyl Cellulose.
FS	Fluid flow scale.
GNF	Generalized Newtonian Fluid.
PAC	Polyanionic Cellulose.
PS	Particle scale.
RPM	Revolutions per minute.

## Symbols

$d$	Diameter.
$g$	Magnitude of gravity.
$L$	Length.
$Q$	Volumetric flow rate.

## Indices

$Cr$	Cross.
$d$	Drag.
$el$	Elastic.
$f$	Fluid, flow.
$h$	Hydraulic.
$i$	Inner.
$mf$	Mean flight.
$o$	Outer.
$p$	Particle.
$PL$	Power Law.
$set$	Settling.
$sr$	Shear rate/Strain rate.
$th$	Thixotropic.

## INTRODUCTION

Polyanionic Cellulose (PAC), as well as its chemical parent sodium Carboxymethyl Cellulose (CMC), is a natural polymer and used both as drilling fluid viscosifier in oil drilling and, dissolved in distilled water, drilling fluid substitute in (experimental) cuttings transport studies. The latter are

typically conducted in research laboratories using flow loops, where a drilling fluid, or a drilling fluid substitute such as the here discussed PAC solutions, is circulated through a, mainly annular, test section of length  $L$  and outer diameter  $d_o$  as depicted in Figure 1.

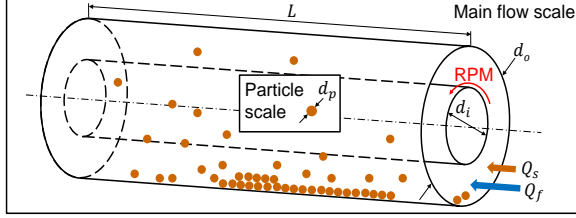


Figure 1: Annular domain typically employed for cuttings transport studies.

The inner pipe with diameter  $d_i$  may rotate with a (not necessarily constant) RPM to replicate drill string rotation and a fluid-particle-mixture characterized by fluid ( $Q_f$ ) and solid ( $Q_s$ ) volumetric flow rates and a particles of mean diameter  $d_p$  are injected at one end to investigate the quality of solids transport through the domain.

#### Problem formulation and paper scope

Typically, PAC solutions are considered purely viscous, i.e. they are rheologically described by a Generalized Newtonian Fluid (GNF) constitutive equation and do neither feature viscoelastic nor time-dependent/shear-history dependent properties. By definition, GNF behaviour implies an instantaneous stress response to a change in shear rate and vice versa. However, PAC solutions do feature both thixotropic and viscoelastic behaviour on time scales ranging from  $10^{-4}$ - $10^1$  and  $10^1$ - $10^3$  s, respectively<sup>1</sup>. It is not clear, under which circumstances the GNF modelling approach is justified for a cuttings transport problem. By means of time scale comparisons in the sense of Deborah<sup>3</sup> and Weissenberg<sup>4</sup> numbers, as well as Pipkin spaces<sup>5</sup>, we investigate the assumption of a GNF for the two relevant spatial scales (see Figure 1), the main fluid flow scale (FS, index  $f$ ) and the particle scale (PS, index  $p$ ). We further

quantitatively validate the GNF assumption for typical parameter ranges for cuttings transport studies.

## MATERIALS & METHODS

### Cuttings transport parameter space

For a cuttings transport problem as depicted in Figure 1, Table 1 provides the relevant (concerning the here discussed rheology of drilling fluid and/or drilling fluid model systems) parameters<sup>6</sup>.

Table 1: Characteristic parameter ranges<sup>6</sup> and cases for problem depicted in Figure 1,  $\rho_f = 1000 \text{ kg/m}^3$  and  $\rho_p = 2650 \text{ kg/m}^3$  for all cases.

	Quantity	#1	#2	#3	#4	#5
FS	$d_o$ [in]	17.5	12.25	9.875	8.5	6.125
	$d_i$ [in]	6.625	6.625	5	4	3.5
	$Q_{f,max}$ [L/min]	5700	4200	3500	2300	700
PS	$d_p$ [mm]	0.01	0.1	1	10	n/a

The apparent viscosity  $\eta_f(\dot{\gamma})$  of PAC solutions is best described with a Cross<sup>7</sup> (Cr) material function<sup>1</sup>

$$\eta_f(\dot{\gamma}) = \eta_\infty + \frac{\eta_0 - \eta_\infty}{1 + (K_{Cr}\dot{\gamma})^{n_{Cr}}} \quad (1)$$

where the Cross model coefficients are given in Table 2 for two different concentrations.

Table 2: Cross material function model parameters for PAC2 (2 g/L) and PAC4 (4 g/L)<sup>1</sup>.

Parameter	PAC2	PAC4	Unit
$n_{Cr}$	0.5162	0.5832	-
$K_{Cr}$	0.0121	0.0278	$\text{Pa}\cdot\text{s}^n$
$\eta_0$	0.0524	0.2121	$\text{Pa}\cdot\text{s}$
$\eta_\infty$	0.0010	0.0010	$\text{Pa}\cdot\text{s}$

### Characteristic time scales of the fluid

In principle, various definitions for characteristic time scales of the fluid, hereafter referred to as rheological times scales, exist. However, for practical simplicity, we here apply two characteristic time scales, namely  $\tau_{el}$  and  $\tau_{th}$ , representing the viscoelastic and thixotropic behaviour of the fluid, respectively. For the PAC solutions

under discussion it was recently shown<sup>1</sup> that they show both viscoelastic and thixotropic behaviour, with relaxation time scale ranges as summarized in Table 3.

Table 3: Characteristic rheological time scales for PAC solutions<sup>1</sup>.

Fluid	$\tau_{el}$ [s]	$\tau_{th}$ [s]
PAC2	0.01...0.23	1.7...76.8
PAC4	0.03...0.29	8.6...615

In principle, one should further distinguish between time scales describing the relaxation of stress for a breaking and for a rebuilding fluid microstructure. For the PAC solutions under discussion, the time scales given in Table 3 are mainly characterising the rebuilding of microstructure. With respect to  $\eta_f$ , 90% of the microstructure build-up happens very fast (<1s), whereas the remaining 10% develop on long time scales (76.8 s, 615 s)<sup>1</sup>.

#### Characteristic time scales of the process

The problem of cuttings transport in drilling, as depicted in a simplified manner for laboratory cuttings transport studies in Figure 1, does occur on various process time scales. For the FS, we define the mean flight (index *mf*) time as a macroscopic time scale on which deformation occurs. This is equivalent to the time it takes an arbitrary fluid element to travel through the domain in the stream wise direction.

$$T_{f,mf} = \frac{L}{U_f} \quad (2)$$

A second characteristic time scale is the inverse of the local rate of deformation/strain rate (index *sr*) and thus associated with the local rate of stretching of an arbitrary fluid element due to imposed shear. It may be estimated by the inverse of the shear rate at the wall of an annulus

$$T_{f,sr} = \frac{D_h}{12U_f} \quad (3)$$

where the narrow-slot approximation is used. On the PS, a characteristic time for the

deformation process is the time it takes the particle to settle its diameter.

$$T_{p,mf} = \frac{d_p}{v_{p,set}} \quad (4)$$

The particle settling velocity  $v_{p,set}$  may be estimated based on Stokes law for  $Re_p < 1$  as

$$v_{p,set} = \frac{(\rho_p - \rho_f) g d_p^2}{18\eta_f}, \quad (5)$$

where in general the average fluid viscosity  $\eta_f(\dot{\gamma})$  at the particle surface, relevant for the particle sedimentation, is a result of a superposition of global strain (the magnitude of the shear rate of the background flow field  $\dot{\gamma}_f$ ) and local strain (the particle-induced shear rate  $\dot{\gamma}_p$ ).

$$\dot{\gamma} = \sqrt{\dot{\gamma}_f^2 + \dot{\gamma}_p^2} \quad (6)$$

For  $Re_p > 1$ , drag laws may be used to estimate the settling velocity, for instance, the empirical expression of Schiller-Naumann<sup>8</sup> for the drag coefficient  $c_d$ , or dedicated GNF drag laws, alternatively.

$$v_{p,set} = \sqrt{\frac{4d_p g}{3c_d} \left(1 - \frac{\rho_f}{\rho_p}\right)} \quad (7)$$

Again, we define a kinematic time scale as the inverse of the shear rate  $\dot{\gamma}_p$ , which for a settling particle is equivalent to the time it takes the particle to settle half its diameter

$$T_{p,sr} = \frac{d_p}{2v_{p,set}}. \quad (8)$$

Another time scale relevant for the case of particle acceleration is the particle relaxation time as the time it takes the particle to adapt to 63 % of the fluids velocity

$$T_{p,rel} = \frac{\rho_f d_p^2}{18\eta_f}. \quad (9)$$

#### Process vs. rheological time scales

A classic relation between characteristic time scales is the concept of the Deborah number

De. The original definition of De is the ratio of a characteristic rheological time scale to the time scale of observation<sup>3</sup>

$$De_{j,i} = \frac{\lambda_i}{T_{Obs}}, \quad i \in \{el, th\}, j \in \{f, p\}. \quad (10)$$

Historically, De is applied to represent the degree of elastic behavior of a material, i.e. whether it predominantly behaves like a fluid or like a solid. Hence, it is considered to describe viscoelastic effects but not time-dependent effects resulting from microstructural changes<sup>9</sup>. However, for the purpose of this study, De serves as a degree of purely viscous behavior, i.e. the assumption of a GNF. For this purpose, De is defined as the ratio of the characteristic rheological time scales of the fluid to the characteristic process time scales of the flow,  $T_{j,mf}$  with  $j \in \{f, p\}$ , i.e. eq. (2) and (4).

The definition of the Deborah number as well as the closely related Weissenberg<sup>4</sup> number

$$Wi_{j,i} = \frac{\lambda_i}{T_{j,sr}}, \quad i \in \{el, th\}, j \in \{f, p\} \quad (11)$$

is not unambiguous. In fact, in the literature varying and unclear definitions exist<sup>9,10</sup>. In contrast to De, which accounts for the degree of transient nature of the flow and becomes zero for Lagrangian and rheologically steady flows ( $T_{Obs} \rightarrow \infty$ )<sup>9,10</sup>, Wi accounts for the degree of non-linear behavior of the material. Note that both De and Wi are functions of the Reynolds number Re because the process time scales depend on the fluid bulk velocity  $U_f = Q_f/A$  or the particle settling velocity  $v_{p,set}$ , the viscosity  $\eta_f$  and a lateral spatial scale, e.g. the particle diameter  $d_p$  or the hydraulic diameter  $d_h = d_o - d_i$ .

## RESULTS

We first present results for the main flow scale followed by results for the particle scale. For both spatial scales, we present results characterising the thixotropic behaviour and the viscoelastic behaviour. Figure 2 and Figure 3 depict the thixotropic

De<sub>th</sub> and Wi<sub>th</sub> as function of the Generalized Reynolds number<sup>11</sup> Re<sub>G</sub> for PAC2 and PAC4, respectively. The power law (PL) coefficients of Re<sub>G</sub> are obtained by requiring  $\eta_f^{PL} = \eta_f^{Cr}$  and  $\partial\eta_f^{PL}/\partial\dot{\gamma} = \partial\eta_f^{Cr}/\partial\dot{\gamma}$  for any given point of the flow curve  $\eta_f = f(\dot{\gamma})$ . Five different ranges are depicted for both De and We on all plots because of: (1) The min. and max. rheological time scales as indicated by Table 3. (2) The different combinations of drill pipe and hole diameters as well as corresponding max. flow rate  $Q_{f,max}$  ( $Q_{f,min}=10$  L/min for all cases) according to Table 1. The length scale  $L$  is estimated with 1 m, which is a typical order of magnitude for the actual development length/test section (Figure 1) of a flow loop. The presented De<sub>th</sub>-Wi<sub>th</sub>-Re<sub>G</sub> spaces are supplemented with the corresponding Pipkin spaces<sup>5</sup>, where De<sub>i</sub> and Wi<sub>i</sub> are plotted in relation to each other (Figure 4, Figure 5). In contrast to the De<sub>i</sub>-Wi<sub>i</sub>-Re<sub>G</sub> spaces, the De<sub>i</sub>-Wi<sub>i</sub> spaces feature only two different lines representing the min. and max. rheological time scales. In the same manner, we subsequently present the viscoelastic behaviour on the main flow scales (Figure 6-Figure 9), the thixotropic behaviour on the particle scale (Figure 10-Figure 13) and the viscoelastic behaviour on the particle scale (Figure 14-Figure 17). The material function  $\eta_f = f(\dot{\gamma})$  predominantly affects Re, rather than De and Wi, which is why the difference in De and Wi is comparatively small for PAC2 and PAC4. On the other hand, De and Wi are strongly dependent on the rheological time scales, which in general are a function of the material function  $\eta_f = f(\dot{\gamma})$ . However, as may be inferred from Table 3, the rheological time scale differences are relatively large for the thixotropic cases but negligible for the viscoelastic cases. For the fluid flow scale, De<sub>el</sub> is of the order <1, while De<sub>th</sub> is of the order  $10^{-2} \dots 10^3$ . In case of the particle scale, De<sub>el</sub> is of the order  $10^{-2} \dots 10^1$ , while De<sub>th</sub>>1 (for  $d_p > 0.1$  mm).

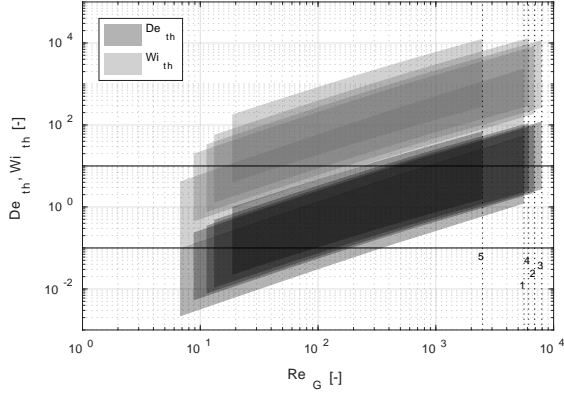


Figure 2.  $\{De_{th}, Wi_{th}\} = f(Re_G)$ , FS, PAC2.

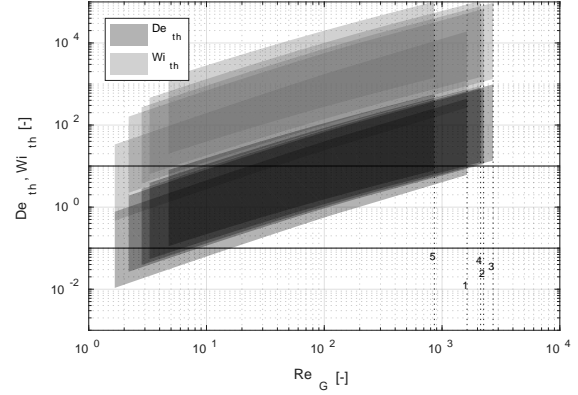


Figure 3.  $\{De_{th}, Wi_{th}\} = f(Re_G)$ , FS, PAC4.

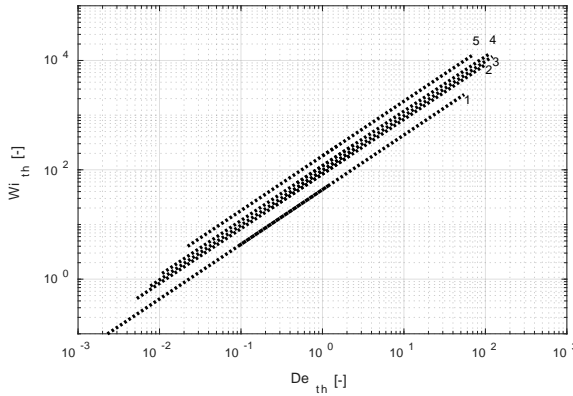


Figure 4.  $Wi_{th} = f(De_{th})$ , FS, PAC2.

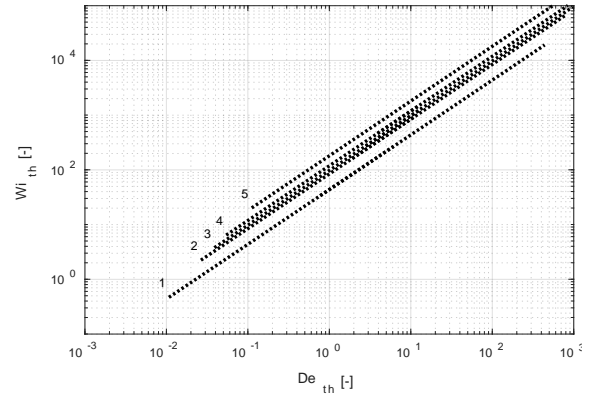


Figure 5.  $Wi_{th} = f(De_{th})$ , FS, PAC4.

With the assumed  $Q_{f,max}$ , transitional flow may be reached on the FS because  $Re_G$  exceeds the turbulent flow threshold 2100. In case of PAC2, particles larger than 1 mm (PAC2) may be expected to deviate from the Stokes flow assumption on the PS because  $Re_p$  becomes larger than 1. In case of PAC4, this happens for  $d_p > 2$  mm.

## DISCUSSION

Pure GNF behaviour is associated with the limit  $De \rightarrow 0$ , i.e. the very left side of the Pipkin space. The  $De$  concept inherently assumes transient development of flow and/or fluid properties, i.e. the process time scale in the denominator describes a transient time scale on which the deformation process evolves. For a steady flow, it is generally argued that the  $De$  loses its meaning. However, in a flow loop the flow is not necessarily Lagrangian steady because of flow unifiers, bends, and pumps.

## Fluid flow scale

Viscoelasticity does not seem to appear a major issue, because  $De_{el} < 0.1$  for the vast majority of the cases investigated. However, for higher polymer concentrations this may be different because the viscoelasticity may be more pronounced. Thixotropy is much more relevant because  $De_{th} > 0.1$  for the majority of the investigated cases. If the flow at the inlet of the test section depicted in Figure 1 is at a full dynamic equilibrium in a Lagrangian sense, i.e.  $\dot{u}_f = 0$ ,  $\dot{\eta}_f = 0$ , and  $\dot{\tau}_f = 0$ , then  $De_i = 0$  and the GNF formulation applies. Other than that, two different cases are to be distinguished: (1) A transient, e.g. start-up flow, where  $U_f$  increases from zero to a nominal value, such as the pump start-up phase in a flow loop. (2) Flows featuring cross-sectional changes and hence a development length  $L$ , for instance because of required pumps or the honeycomb-like

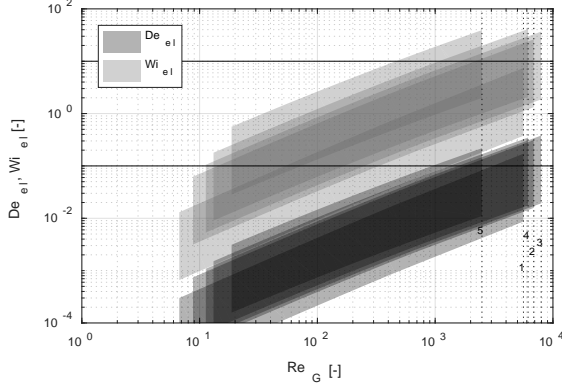


Figure 6.  $\{De_{el}, Wi_{el}\} = f(Re_G)$ , FS, PAC2.

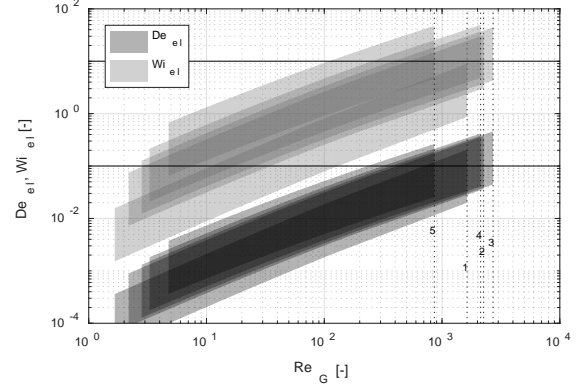


Figure 7.  $\{De_{el}, Wi_{el}\} = f(Re_G)$ , FS, PAC4.

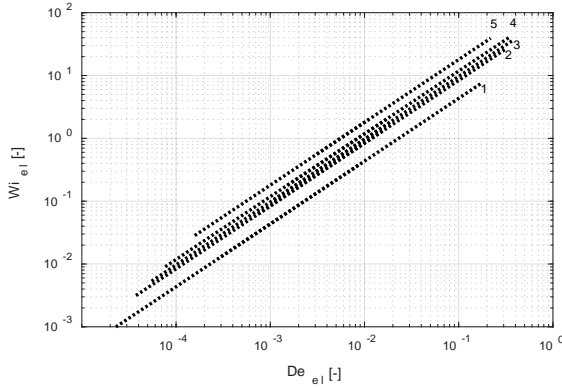


Figure 8.  $Wi_{el} = f(De_{el})$ , FS, PAC2.

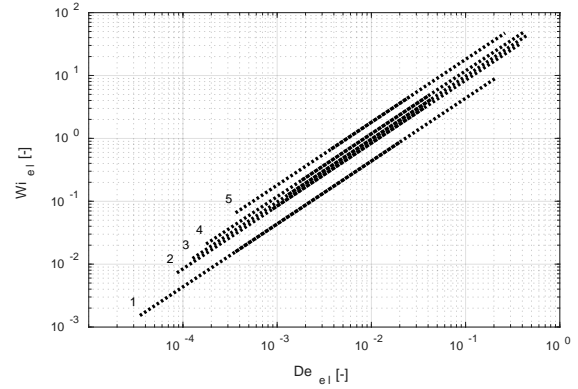


Figure 9.  $Wi_{el} = f(De_{el})$ , FS, PAC4.

flow straighteners often used in flow loops prior to the test section where quantities of interest are measured.

Lagrangian steadiness requires different measures for ensuring these two cases:

- (1)  $U_f \neq U_f(t) \leftrightarrow \text{Increase } T_{obs}$
- (2)  $U_f \neq U_f(L) \leftrightarrow \text{Increase } L$

These measures will shift the characteristic line in the Pipkin space towards the GNF regime. However, the flow must also be rheologically steady, i.e. no microstructure break-down and-build up must occur. This may even require larger observation times and/or development lengths than what is required to obtain e.g. constant/fully developed velocity profiles. A particular example is the fluid residence time in the flow loop section between the pump and the test section vs. the rheological time scales. The mean viscosity is to some extent defined by the pump rather than the wall shear in the

test section if the distance pump to test section is not sufficiently long. Alternatively, tanks may be utilized to store certain amounts of fluid after the pump and allow for structural recovery.

Obviously, both increasing  $T_{obs}$  and  $L$  is restricted by laboratory constraints; hence, a trade-off analysis is required which provides an estimate of the error for the given laboratory setup and assumed GNF behaviour. For the considered PAC solutions, the relative difference between the in-situ apparent viscosity and a GNF assumption, i.e. the equilibrium flow curve, may be in the order of 10...20% for a (comparatively large) step in shear rate (0.1 1/s to 1200 1/s and back)<sup>1</sup>, depending on  $T_{obs}$ . The issue of microstructural change on longer time scales in the order of  $10^3$  s is also a problem when obtaining flow curves. Sufficient time must be allowed for a particular shear rate-

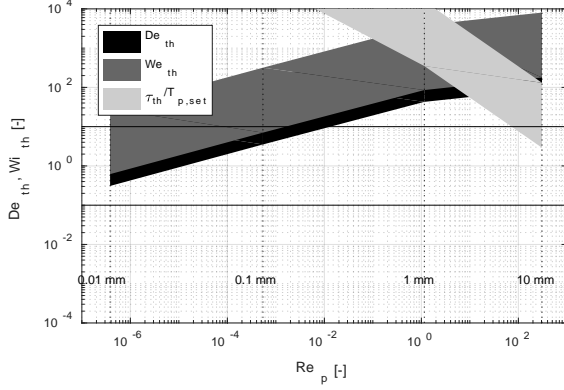


Figure 10.  $\{De_{th}, Wi_{th}\} = f(Re_G)$ , PS, PAC2.

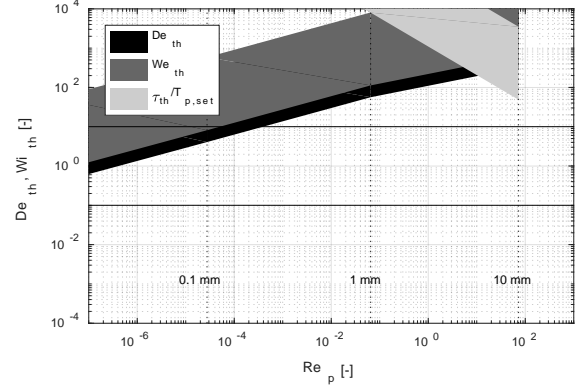


Figure 11.  $\{De_{th}, Wi_{th}\} = f(Re_G)$ , PS, PAC4.

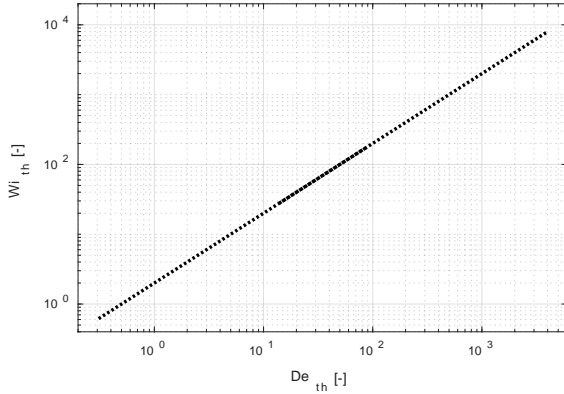


Figure 12.  $Wi_{th} = f(De_{th})$ , PS, PAC2.

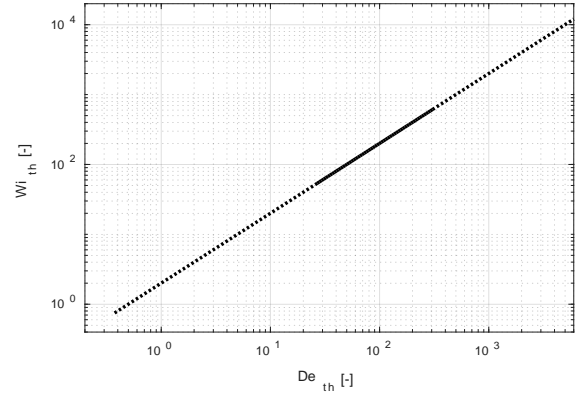


Figure 13.  $Wi_{th} = f(De_{th})$ , PS, PAC2.

apparent viscosity reading to obtain a full dynamic equilibrium and the true steady state apparent viscosity<sup>1</sup>.

Care must be taken when reporting results in purely non-dimensional form. For higher  $Re_G$ , viscoelastic effects in the form of normal stress differences become relevant and should be accounted for in the definition of  $Re_G$ <sup>12</sup>.

#### Particle scale

For a single particle  $> 0.1$  mm settling in a quiescent PAC solution,  $De_{el}$  are in the range 0.1...10. This indicates that the effect of elastic wake and, for larger particles  $> 2$  mm, the effect of particle acceleration may have a significant influence on the particle drag. The elastic effect on drag may be accounted for by the application of a viscoelastic correction to the drag coefficient<sup>13</sup> and thus keeping the GNF formulation.

For a single particle  $> 0.1$  mm settling in a quiescent PAC solution,  $De_{th}$  are larger than 10. At first glance, this indicates that the effect of microstructural changes may not fully affect the particle drag of a particular particle because  $\eta_f(\dot{\gamma})$  is far from equilibrium. However, for the PAC solutions investigated, the time scales on which microstructure breakdown occurs are very much shorter than the microstructure build-up time scales<sup>1</sup>. Hence, more data for the actual time scales on which microstructure breakdown occurs is required. For the more generic case of an orthogonal shear flow, such as a particle settling in steady annular flow,  $\dot{\gamma}$  is typically evaluated according to equation (6). Typically, drag laws are purely reported in the non-dimensional form  $c_D = f(Re_p)$ . Again, care must be taken to use the actual viscosity as seen by the particle and/or provide the error range based on the viscosity

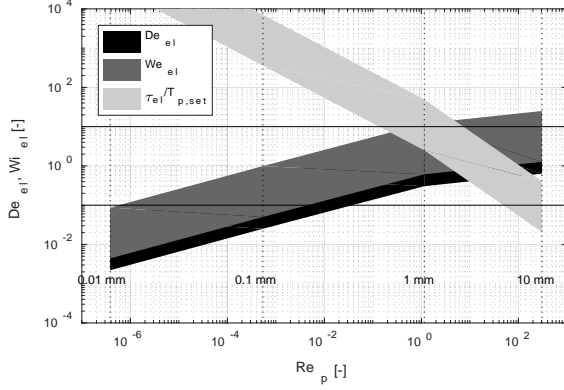


Figure 14.  $\{De_{el}, Wi_{el}\} = f(Re_G)$ , PS, PAC2.

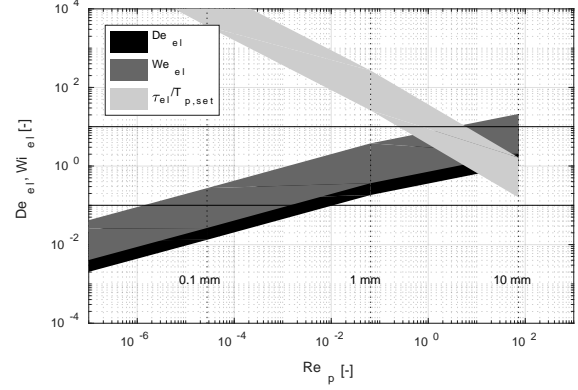


Figure 15.  $\{De_{el}, Wi_{el}\} = f(Re_G)$ , PS, PAC4.

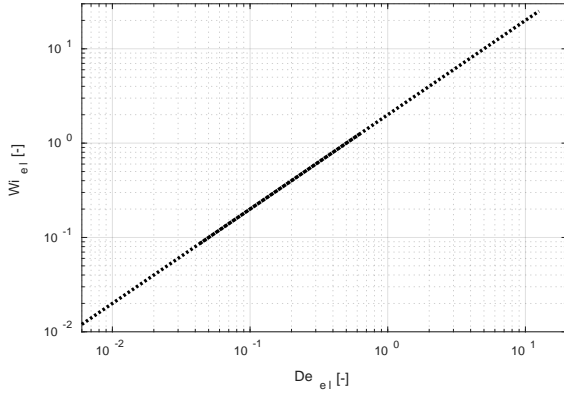


Figure 16.  $Wi_{el} = f(De_{el})$ , PS, PAC2.

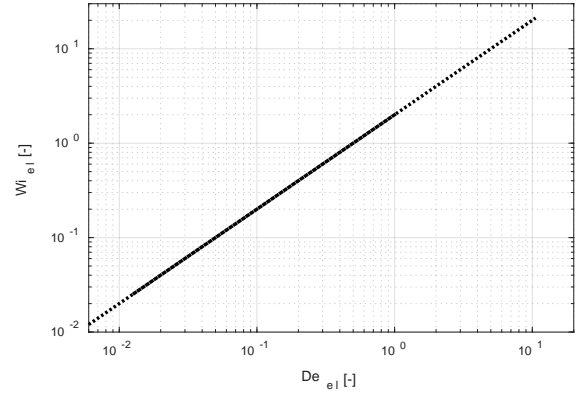


Figure 17.  $Wi_{el} = f(De_{el})$ , PS, PAC4.

range  $\eta_0 \dots \eta_f$  ( $\dot{\gamma}_p$ ) and the rheological time scales.

Particles following in the wake of a settling particle may see the altered fluid microstructure and hence experience a lower or even larger apparent viscosity<sup>1</sup>. As a GNF, i.e. instantaneous, response to the induced shear rate is assumed, the non-equilibrium rheological state may lead to an  $\dot{\gamma}_p$  error ( $\approx 10\%$ )<sup>1</sup> for  $De_{th} > 10$ . The error is more severe the smaller  $\dot{\gamma}_f$ , i.e. the more quiescent the fluid is, for instance in the centre of the velocity field or when determining drag laws via settling experiments. In addition, on a larger scale, multiple particles will lower the fluids viscosity for the thixotropic periods given in Table 3.

For larger particles, particle acceleration is affected by the fluids rheological properties because the ratios  $\tau_i/T_{p,rel}$  are approaching

unity for larger particles ( $d_p > 1$  mm and  $d_p > 0.1$  mm for  $\tau_{th}$  and  $\tau_{el}$ , respectively).

#### Transitional flows

For the FS, transitional flows occur for higher velocities as  $Re_G$  exceeds 2100 (Figure 2, Figure 3). Here, turbulent drag (wall friction) reduction may be expected because the elasticity number<sup>14</sup>  $El$  as the ratio of  $Wi_{el}$  and  $Re$  is in the order of  $10^{-3} \dots 10^{-2}$  (the latter being the magnitude for large  $U_f$  values) and a threshold for drag reduction<sup>14</sup> is  $\sqrt{El} \approx 0.0065$ .

One may also expect some thixotropic effects to be present in the higher  $Re_G$  regions (Figure 2, Figure 3). A classical turbulent time scale is the large eddy turnover time  $d_h/U_f$ , i.e. equation (3) multiplied with 12, hence, a  $De$  based on the thixotropic time scale and the large eddy turnover time would still be significantly larger than unity.



Furthermore, in the transitional flow regime, the viscosity  $\eta_f$  and, following a Reynolds-Averaged Boussinesq<sup>15</sup> approach, the turbulent viscosity do have the same order of magnitude.

## CONCLUSIONS

For the PAC solutions considered here, the GNF assumption does not hold for all investigated cases. Increasing observation times and flow development length as well as utilizing tanks to allow for structural recovery are measures that can be taken to ensure that experimental data is sampled at dynamic equilibrium for which the GNF formulation is valid.

If results are reported in non-dimensional form, a flow-kinematic-dependent error in the order of 10% may be induced if the, in fact time-dependent, viscosity is simply based on a GNF constitutive equation.

## ACKNOWLEDGEMENTS

The project [Advanced Wellbore transport Modeling \(AdWell\)](#) with its sponsor, PETROMAKS 2/the Research Council of Norway (project 228391) and its partners Statoil, Neptune Energy Norge AS, IRIS, UiS, NTNU and SINTEF are gratefully acknowledged for funding and supporting this work. Further, we thank our colleagues Aminul Islam (Statoil) and Dwayne Martins (Neptune Energy Norge AS) for reviewing the paper and providing valuable input.

## REFERENCES

1. Busch, A. *et al.* (2018), "Rheological characterization of Polyanionic Cellulose solutions with application to drilling fluids and cuttings transport modeling", *Applied Rheology* **28**, 1–16.
2. Ad Hoc Committee on Official Nomenclature and Symbols. (2013), "Official symbols and nomenclature of The Society of Rheology", *Journal of Rheology* **57**, 1047–1055.
3. Reiner, M. (1964), "The Deborah Number", *Physics Today* **17**, 62.
4. White, J. L. (1964), "Dynamics of viscoelastic fluids, melt fracture, and the rheology of fiber spinning", *Journal of Applied Polymer Science* **8**, 2339–2357.
5. Pipkin, A. C. (Springer-Verlag, 1986), "*Lectures on viscoelasticity theory*".
6. Busch, A. *et al.* (2018), "Cuttings Transport Modeling - Part 1: Specification of Benchmark Parameters with a Norwegian Continental Shelf Perspective", *SPE Drilling & Completion* **preprint**.
7. Cross, M. M. (1965), "Rheology of non-Newtonian fluids: a new flow equation for pseudoplastic systems", *Journal of colloid science* **20**, 417–437.
8. Schiller, L. *et al.* (1933), "Über die grundlegenden Berechnungen bei der Schwerkraftaufbereitung", *Z. Ver. Dtsch. Ing* **77**, 318–320.
9. Dealy, J. M. (2010), "Weissenberg and Deborah Numbers - Their Definition and use", *Rheology Bulletin* **79**, 14–18.
10. Poole, R. J. (2012), "The Deborah and Weissenberg numbers", *The British Society of Rheology, Rheology Bulletin* **53**, 32–39.
11. Metzner, A. B. *et al.* (1955), "Flow of non-newtonian fluids-correlation of the laminar, transition, and turbulent-flow regions", *AIChE Journal* **1**, 434–440.
12. Harris, J. (1963), "A note on the generalized Reynolds number in non-Newtonian flow", *British Journal of Applied Physics* **14**, 817.
13. Acharya, A. *et al.* (1976), "Flow of inelastic and viscoelastic fluids past a sphere - I. Drag coefficient in creeping and boundary-layer flows", *Rheologica Acta* **15**, 454–470.
14. Denn, M. M. *et al.* (1971), "Elastic effects in flow of viscoelastic liquids", *The Chemical Engineering Journal* **2**, 280–286.
15. Boussinesque, J. (1877), "Essai sur la theories des eaux courantes, Memoires presentes par divers savants a l'Academic des Sciencede l'Institut National de France", *Tome XXIII*.